Transient receptor potential vanilloid 4 (TRPV4) channels mediate pulmonary surfactant protein A and D secretion

Philipp Alt[1], Isabel Müller[1,5], Martina Kiefmann[1,5], Thomas Gudermann[1,5], Wolfgang M. Kuebler[2], Matthias Griese[3,5], Claudia A. Staab-Weijnitz[4,5], and Alexander Dietrich[1,5]

[1]Walther Straub Institute of Pharmacology and Toxicology, Medical Faculty, LMU-Munich, Munich Germany.

[2]Institute of Physiology, Charité - Universitätsmedizin Berlin, Berlin, Germany

[3]Department of Pediatrics, Dr. von Hauner Children's Hospital, University Hospital, LMU-Munich, Munich, Germany

[4]University of Colorado, Anschutz Medical Campus, Department of Pediatrics and Division of Pulmonary Allergy and Critical Care Medicine, School of Medicine, Aurora, CO, USA

[5]Deutsches Zentrum für Lungenforschung (DZL), CPC-M, Munich, Germany

Running title: TRPV4 in SP-A, -D secretion and differentiation

Conflict of interest: The authors have declared that no conflict of interest exists.

Address correspondence to: Alexander Dietrich, Walther-Straub-Institute of Pharmacology and Toxicology, Medical Faculty, LMU-Munich, Nussbaumstr. 26, 80336 Munich, Germany. Phone + 49 89 2180 73802; Fax + 49 89 2180 73817, Email: Alexander.dietrich@lrz.uni-muenchen.de, ORCID ID: 0000-0002-1168-8707

Author Contributions: P.A., W.M.K., and A.D. conceived of the main conceptual idea. P.A., and I.M. carried out the experiments. P.A., I.M., T.G., W.M.K., M.G., C.S.-W., and A.D. performed critical analysis of the data. P.A. and A.D. wrote the manuscript. All authors discussed the results and contributed to the final manuscript**.**

Keywords: AT2 cells, club cells, surfactant protein secretion, human and mouse air-liquid-interface models

An **AI tool** was not used for the production of this manuscript.

Clinical relevance: Our data provide evidence for an essential role of TRPV4 channels in secretion of surfactant protein A and -D in the alveolus and the murine and human tracheobronchial tree. TRPV4 protein might enhance SP-A and -D secretion for a more powerful immune response.

This article has a data supplement, which is accessible at the Supplements tab.

Abstract

Lung surfactant reduces not only surface tension at the air liquid interface, but is also involved in pulmonary host defense. This important role in innate immunity of the respiratory tract is primarily mediated by surfactant proteins A and D (SP-A, -D), which are secreted from alveolar epithelial type 2 (AT2) cells and from tracheal and bronchial epithelial cells expressing Transient Receptor Potential Vanilloid 4 (TRPV4) channels. In a mouse model deficient in TRPV4, reduced levels of SP-A and SP-D were detected in the bronchoalveolar lavage (BAL) fluid. Production of both proteins in TRPV4-/- AT2 cells was not different to wild-type control cells, but secretion of SP-A and -D was impaired both in TRPV4-deficient murine AT2 and in murine tracheal epithelial cells (MTEC) cultured at the air liquid interface (ALI). In a translational approach, we established a human ALI model and differentiated bronchial basal cells to a pseudostratified epithelium. Downregulation of *TRPV4* mRNA expression by specific siRNAs also resulted in a reduction of secreted SP-A levels. Interestingly, differentiation of basal cells to ciliated cells, but not club cells, which secrete SP-A and -D, was decreased after down-regulation of TRPV4. Our data highlight novel essential functions of TRPV4 channels in secretion of SP-A and SP-D, which are important not only for innate immunity, but also for lung diseases like asthma and Idiopathic Pulmonary Fibrosis (IPF).

Introduction

Our respiratory tract is responsible for gas exchange, but also must be protected from invading pathogens. To facilitate both, distal pulmonary tissues produce a fluid called lung surfactant. This surfactant is mainly composed of lipids, but also contains a total of 8% of surfactant proteins A-D (SP-A, -B, -C, -D) (1). While SP-B and -C are hydrophobic and strongly interact with the phospholipid bilayer of the surfactant (2), which is essential for surface tension reduction and efficient gas exchange in the alveoli of the lungs, the more hydrophilic SP-A and -D bind to apoptotic cells (3, 4) and a variety of bacteria as well as viruses, including SARS-CoV-2 (5). Coupling to these pathogens will result in lysis, increased phagocytosis and production of cytokines as well as reactive species by immune cells (4, 6, 7). Along this line, increased broncho-alveolar levels of SP-D have been demonstrated in children with asthma or recurrent bronchitis, while patients with an SP-D deficiency suffered from pneumonia (8). Recently, roles for SP-A in asthma (9), lung repair by macrophages (10) and synergistic actions with antibiotics against gram-negative respiratory bacteria (11) were reported, while SP-D is involved in tumor immunoregulation (12). Both SPs contribute to phagocytosis of nanomaterials by macrophages (13) and are associated with infections by Respiratory Syncytial virus (RSV) in children (14), Idiopathic Pulmonary Fibrosis (IPF) and Hypersensitivity Pneumonitis (HP) (15). All four SPs are produced in alveolar epithelial type 2 (AT2) cells, but SP-A and -D are also synthesized and secreted in the tracheal-bronchial region by club and submucosal cells (16) as well as in extrapulmonary tissues (3). The tracheal and bronchial regions of the airways enable the removal of pathogens and debris by mucociliary clearance (reviewed in (17)). While goblet cells mainly produce mucins, which form mucus for the mucociliary movement by ciliated cells, club cells are also able to secret SP-A and -D for an

efficient removal of invading pathogens (18). Along these lines, mouse models deficient in SP-A and SP-D expose a defective or altered response after a challenge with bacterial, fungal or viral microorganisms or to bacterial lipopolysaccharides *in-vivo* (reviewed in (18)).

Transient receptor potential (TRP) channels, originally cloned *in Drosophila melanogaster*, serve multiple functions in different mammalian tissues (19) including the lung (20). Transient receptor potential vanilloid 4 (TRPV4) is the fourth member of the vanilloid family of TRP channels (21). Like most TRP channels, TRPV4 harbors an invariant sequence, the TRP box (containing the amino acid sequence: EWKFAR), in its intracellular C-terminal tail as well as ankyrin repeats in the intracellular N-terminus. The protein is composed of six membrane-spanning helices (S1-6), and a presumed pore-forming loop between S5 and S6 (21, 22). Four of these monomers of the same type preferentially assemble in a functional homo-tetrameric complex (23), although in cell cilia of renal epithelial cells TRPV4/TRPP2 complexes were also identified (24). Homo-tetrameric TRPV4 was originally characterized as a sensor of extracellular osmolarity (25, 26). The channel is functionally expressed in endothelial (27, 28) and epithelial cells of the respiratory system (29-31). TRPV4 channels may serve as mechanosensors because they are activated by membrane and shear stretch as well as by viscous loading (32). Along this line, TRPV4 channels regulate ciliary beat function for mucociliary clearance by ciliated cells (29) and are involved in pulmonary hypertension (33, 34). Moreover, TRPV4-/- mice were protected from bleomycin-induced pulmonary fibrosis due to the channel's constitutive expression and function in lung fibroblasts (35). Therefore, the channel is an interesting pharmacological target and numerous modulators have already been identified (reviewed in (36)).

In this study, we identified reduced SP-A and SP-D levels in the bronchoalveolar lavage (BAL) fluid from TRPV4-/- mice, which was not due to a decreased production in AT2 cells, but to a reduced secretion from AT2 cells and from differentiated mouse tracheal epithelial cells (MTEC). In a translational approach, we utilized a human ALI model to reproduce reduced SP-A and -D expression in the bronchial region after down-regulation of TRPV4 channels. Moreover, differentiation of ciliated cells, but not goblet and club cells were reduced after TRPV4 down-regulation. Therefore, our data suggest essential roles of TRPV4 channels in AT2 cells and the bronchial epithelium for the secretion of SP-A and -D.

Methods

Animals

TRPV4-/- (B6.199X1-Trpv4^{tm1MSZ} from Riken BioResource Center (RBRC01939) (37, 38) were backcrossed 10 times to the C57/BL6J strain. Male and female mice 3 months of age were used in the experiments, if not mentioned otherwise in the figure legends. All animal experiments were approved by the local authority (Regierung Oberbayern).

Human ALI model

Human bronchial epithelial cells (NHBECs) from healthy donors were obtained from Lonza (Basel, Switzerland, CC#2540S, see Supplemental Table E1 for donor information). Ethics statements were provided by the supplier. Cells were expanded for a maximum of three passages (Rayner, Makena, Prasad, & Cormet-Boyaka, 2019) in PneumaCult™Ex Plus medium and were seeded onto 12-well Transwell™-inserts (100,000 cells/insert) with collagen IV (Sigma Aldrich, Germany, #C6745) coating. They were kept at 37 °C and 5 % CO2 and air-lift was performed 2-3 days after seeding when confluency was reached. The medium at the basal compartment was changed to PneumaCult™ ALI-medium and, from then, medium change was performed every two days. Cells were washed once a week to remove secreted mucus and wash-offs were collected for further analysis. Depending on the experimental setup, cells were cultured for 7, 14, 21, 28 or 35 days.

Transient knockdown of TRPV4 in human bronchial epithelial cells

The transfection of human bronchial epithelial cells with specific siRNAs (Horizon Discovery, UK, TRPV4 smartpool, #L-004195-00-005) against TRPV4 was performed using siRNA (Supplemental Table E2, 3) at a final concentration of 10 nM in a mix of

OptiMEM™ (Gibco, Thermo Fisher Scientific, USA, #31985070) and Lipofectamine™ RNAiMAX (Thermo Fisher Scientific, #13778030), which was applied to the apical side of the inserts with seeded cells in submerged culture with PneumaCult™ExPlus medium. After transfection time of 8 h, medium was changed on both sides of the insert and cells were incubated at 37 °C with PneumaCult™ExPlus medium until air-lift was performed. Successful transfection was validated via Western Blot with samples taken 3 days, 5 days and 10 days after treatment. Cells were cultured and differentiated as described above.

Proximity Ligation Assay (PLA)

To confirm findings of the Co-IP experiments in the surfactant producing cells, AT2-cells were isolated from mice and fixed 24h after isolation with 4% PFA solution. The cells were treated according to the steps of the manufacturer´s protocol. In brief, cells were blocked in blocking solution and incubated with primary antibodies (from different hosts) against SP-A and TRPV4 or SP-D and TRPV4. Then, PLA-probes and ligation buffer for rolling circle amplification were added. After amplification step and incubation with fluorescent-labeled oligonucleotide probes (complementary to the amplified product), cells were washed and mounted in DAPI-containing mounting-medium (Merck, Germany, anti-mouse MINUS #DUO92004-30RXN, anti-rabbit PLUS #DUO92002-30RXN, anti-goat PLUS #DUO92003-30RXN, Duolink® In Situ Mounting Medium #DUO82040-5ML, see also Supplemental Table E5). For experiments shown in Supplemental Figure E5, plasma membranes of cells were additionally stained with a fluorescent coupled E-Cadherin ((anti-CD324)) Thermo Fisher Scientific, Waltham, Massachusetts, USA, #53-3249-82) antibody. After solidifying overnight, the cells were imaged with the respective channel with a confocal microscope (LSM 880, Zeiss, Germany).

Statistical analysis

For statistical analysis, GraphPad Prism 10 software (GraphPad Software, San Diego, USA) was used. Significant differences are indicated by asterisks. All data are represented as means + SEM.

All other methods are described in the data supplement.

Results

Ablation of TRPV4 decreases amounts of surfactant protein A and D (SP-A, -D) in murine lung lysates and the bronchoalveolar lavage (BAL) fluid, due to decreased secretion but not to changes in their synthesis in alveolar type 2 (AT2) cells.

To investigate the role of TRPV4 in the production and secretion of SP-A and SP-D, we isolated lungs from wild-type (WT) and TRPV4-deficient (TRPV4-/-) mice. A quantitative Western-Blot analysis of whole lung lysates revealed significantly reduced levels for both surfactant proteins in TRPV4-/- mice compared to WT controls (Figure 1A, B). We next analyzed the content of both proteins in BAL fluids. As volumes of BAL fluid correlate with lung volumes, we performed *in-vivo* lung function measurements of WT and TRPV4-/- mice and were able to exclude any changes in total lung volumes as well as lung volumes normalized to body weights (Figure 1C, D). SP-A and SP-D levels were significantly decreased in BAL fluids of TRPV4-/- mice compared with WT control animals (Figure 1E, F). While sex specific differences for both SP levels were not observed in WT and TRPV4-/- mice (see Supplemental Figure E1), only SP-A and -D levels in lung lysates of females were not significantly different in TRPV4-/- compared to WT lungs (see Supplemental Figure E2) for yet unknown reasons. To further investigate the role of TRPV4 channels for the production of surfactant proteins,

we isolated surfactant producing AT2 cells as described (39), After identification of primary AT2 cells by its primary marker protein pro-surfactant protein C (Figure 2A-C), we performed Ca^{2+} imaging experiments with fully differentiated AT2 cells identified by staining lamellar bodies with LysoTracker DND 26 (Supplemental Figure 3A) using a TRPV4 activator (GSK 1016790A, Supplemental Figure 3B) and preincubation with a TRPV4 inhibitor ((HC0974047 Supplemental Figure E3C) to verify again functional expression of TRPV4 channels in these cells. TRPV4 protein was not detectable in AT2 cells isolated from TRPV4-/- mice (Supplementary Figure E4), which showed no gross morphological changes compared to WT cells. However, expression of both surfactant proteins SP-A and SP-D was not decreased in AT2 cells from TRPV4-/- mice compared to WT mice (Figure 2D, E). Therefore, we quantified SP-A and SP-D levels in the supernatant of primary AT2 cells by ELISA and detected significant less protein secreted by TRPV4-deficient cells compared to WT controls (Figure 2F, G).

TRPV4 channels interact with SP-A and SP-D proteins in primary murine AT2 cells.

As both proteins are secreted independently from lamellar bodies (40, 41) in clear contrast to SP-B and SP-C, we next tested a possible interaction of TRPV4 channels with SP-A and SP-D, which might facilitate secretion of both proteins from AT2 cells. We first utilized a heterologous overexpression system in HEK293 cells and co-immunoprecipitated TRPV4 channels with flag tagged SP-A and SP-D and vice versa using a specific TRPV4 antiserum and a flag antibody, respectively (Figure 3A-D). While both proteins were co-immunoprecipitated with a TRPV4 antiserum as well as TRPV4 channels by antibodies directed against the flag tag of both SPs, another channel, TRPC6, was not able to interact with SP-A and D (Supplementary Figure E5). To confirm these results in primary AT2 cells we used a Proximity Ligation Assay

(PLA), which allows detection of single protein-protein interaction by a fluorescence signal in primary cells (42) with two specific antibodies detecting SP-A and D in AT2 cells (Supplementary Figure E6). PLA-Technology uses a pair of secondary antibodies tagged with oligonucleotides, which if localized within 40 nm in a cell initiates a rolling circle amplification to be detected by fluorescence-coupled probes. Indeed, both SP-A and D colocalized with TRPV4 channels in primary AT2 cells detected by fluorescence signals in WT, but not in TRPV4-defient cells (Figure 3E). To further localize this interaction of SP-A or SP-D with TRPV4 channels in AT2 cells we used an E-cadherin antibody as a marker of cell plasma membranes after performing a PLA. Most interestingly, almost all PLA signals were localized intracellular and not at the plasma membrane (Supplemental Figure E7). Therefore, TRPV4 channels might facilitate SP-A and SP-D secretion by physically interacting mostly in intracellular compartments.

TRPV4 deficiency decreases amounts of surfactant protein A and D (SP-A, -D) in mucous layers of murine tracheal epithelial cells (MTEC) differentiated in an Air-Liquid-Interface (ALI) model.

Next to AT2 cells, surfactant proteins, especially SP-A and -D, are also produced and secreted in club cells of the human tracheal and bronchial regions (43, 44). To quantify surfactant protein production in these cells, we first isolated MTEC from WT and TRPV4-/- mice and seeded them on cell culture inserts for expansion and differentiation in an ALI model to ciliated and club cells as described ((45), Figure 4A, B). We detected no gross morphological changes in the differentiation of TRPV4-/- MTEC compared to WT cells. Again, quantification of SP-A and SP-D expression in cell lysates from ALI-differentiated cells revealed no differences (Figure 4C-F). However, in mucous layers secreted from TRPV4-/- cells analyzed by Western-Blotting we identified significantly lower SP-A and SP-D levels compared to WT controls

(Figure 4C-F). Therefore, secretion but not production of SP-A and SP-D is reduced by ablation of TRPV4 channels in the tracheal region.

Downregulation of TRPV4 channels inhibits secretion of surfactant protein A (SP-A) and basal cell differentiation to ciliated cells in an air liquid interface (ALI) model of human bronchial epithelial cells (HBEC).

In a translational approach, we established a human ALI model (Figure 5A) using bronchial epithelial cells (46) from three healthy human donors (see Table E1). The differentiation process to a pseudostratified epithelium was evident in cross sections by an increasing thickness of the attached cell layer and the appearance of cilia (indicated by white arrowheads on day 14 after the air-lift, Figure 5B). We again detected no gross morphological differences in TRPV4-/- cells compared to WT HBEC. As human basal cells next to ciliated cells express high amounts of TRPV4 mRNA ((47), data published on www.ipfcellatlas.com), we set out to down-regulate TRPV4 expression with specific siRNAs at an early (Transfection 1 with the initial seeding of basal cells on inserts 3 days before air-lift) or a late time point (Transfection 2 after final differentiation to a pseudostratified epithelium 28 days after air lift) (Figure 5A). We reasoned that at the earlier time point we would be able to identify a role for TRPV4 channels in the differentiation of basal cells to SP-A and SP-D secreting club cells, and at the later time point we would test for TRPV4 function in SP-A and SP-D secretion to the mucous layer. By adding a TRPV4 specific siRNA with the transfection reagent to the medium in the upper compartment during the initial seeding of basal cells in inserts, we were able to suppress TRPV4 protein production by 93, 89 and 71 ± 4 % on day 2, 5 and 10 after transfection, respectively (Supplemental Figure E8A, B). TRPV4 protein production was also significantly down-regulated 14, 21 and 28 days after transfection with a TRPV4 specific siRNA (Supplemental Figure E8C). TRPV4 mRNA expression

also increased during differentiation and was already not significantly different any more at day 28 (Supplemental Figure E9). To test for functional expression of TRPV4 channels in human basal cells, we again performed Ca^{2+} imaging experiments with a TRPV4 activator (GSK 1016790A) and a TRPV4 inhibitor. While untransfected and control transfected cells showed a clear increase in intracellular Ca2+ levels after adding a TRPV4 channel activator (Supplemental Figure 10A, B), which was abolished by a TRPV4 inhibitor (Supplemental Figure 10B), TRPV4 siRNA transfected cells showed no changes (Supplemental Figure 10C). Next, we quantified cell numbers by using specific fluorescence-coupled antibodies (ab) for four cell types (Figure 6A, B). While numbers of club (marked by CC10 ab) and ciliated cells (marked by acetylated α-tubulin ab) increased during the differentiation process as described (48, 49), Figure 6D, F), the amount of goblet cells (marked by MUC5AC ab) stayed at a low level (Figure 6E). We detected a lower number of basal cells at day 7 and a higher number of club cells at day 28 in cells transfected with the TRPV4-specific siRNAs compared to the control siRNAs. However, in clear contrast to the other cell types, numbers of ciliated cells were significantly decreased after down-regulation of TRPV4 channels on day 14, 21 and 28 by a TRPV4 specific siRNA in comparison to control siRNAs added during seeding of basal cells to the filter inserts (Figure 6B, F). Along this line, acetylated α-tubulin levels normalized to control cells were also decreased after down-regulation of TRPV4 on day 14 and 28 after air-lift (Supplemental Figure E11A), while total levels increased during basal cell differentiation (Supplemental Figure E11B). Most interestingly, total cell counts (Figure 6G) and number of basal cells (Figure 6C) were not significantly different after down-regulation of TRPV4 channels compared to controls at day 28 after air lift pointing to a differentiation block of ciliated cells but not a complete loss of cells in the absence of TRPV4 protein.

As production of TRPV4 protein by siRNA-mediated down-regulation partially and fully recovered on protein (Supplemental Figure E8A-D) and mRNA level (Supplementary Figure E9) 28 days after air lift, respectively, we chose an alternative later transfection time point to study the role of TRPV4 channels on SP-A and SP-D levels in differentiated human bronchial epithelial cells 28 days after air-lift (Figure 5A). TRPV4 channel protein expression was indeed significantly down-regulated at day 35 after air lift after application of TRPV4 specfic siRNAs at this later time point (Supplemental Figure 12A, B). While levels of both surfactant proteins were not different in cell lysates with down-regulated TRPV4 channels (Figure 7A), SP-A proteins were significantly reduced in mucous layers washed off from cell layers (Figure 7C) 7 days after air lift and recovered to normal levels 14 days after air lift. A successful down-regulation of TRPV4 channels at a later time point (day 28, see Supplementary Figure E6A, B) was however again successful in reducing SP-A levels 35 days after airlift in the mucous layer (Figure 8D), but not in cell lysates (Figure 7B). While our ELISA was not sensitive enough to detect SP-D levels in mucous layers, SP-D levels in cell lysates at day 35 after air lift were again not significantly different (Figure 7E) similar to SP-A levels (Figure 8B). In contrast to murine AT2 and tracheal epithelial cells (MTEC) as well as human bronchial epithelial cells, TRPV4 proteins were not detected in AT2 cell supernatants, murine and human mucous layers (Supplemental Figure 13A, B).

Thus, lower SP-A and SP-D levels in bronchial fluids are not due to lower cell numbers of club, nor to the production in these cells. Similar results were obtained from the TRPV4-deficient mouse model (Figure 1, 2). Therefore, our findings provide evidence for an important role of TRPV4 channels in secretion of SP-A and SP-D in the pseudostratified epithelium.

4. Discussion

TRPV4 channels are expressed in different tissues of the respiratory tract. They play an important role in fibroblast-to-myofibroblast differentiation during the progression of pulmonary fibrosis (35) and endothelial barrier function for immune cell invasion (reviewed in (50)). But their exact function in the lung alveolus and tracheobronchial epithelium is still elusive (reviewed in (20, 51)). We recently identified TRPV4 function in AT1 and AT2 cells of the lung alveolus (39). Ablation of TRPV4 channels resulted in a decreased production of pro-surfactant protein C (pSP-C) in AT2 and lower aquaporine 5 (AQP-5) expression and membrane localization in AT1 cells, which were most likely responsible for emphysema like changes in older mice and an increased ischemia-reperfusion induced edema formation, respectively (39).

Here, we quantified two other surfactant proteins, SP-A and SP-D, in the same TRPV4-/- mouse model. In contrast to SP-B and SP-C, which closely interact with phospholipids and are integral members of the surfactant, SP-A and SP-D are secreted independent of lamellar bodies (40, 41), bind to pathogens and are essential for a strong innate immunity (3, 4, 6, 7, 18). Most interestingly, levels of both proteins were significantly reduced in lung lysates and BAL-fluids of TRPV4-/- mice in comparison to WT controls (Figure 1A, B and E, F), while production was normal in AT2 cells *in-vitro* (Figure 2D, E). However, SP-A and SP-D levels in the supernatant of TRPV4-deficient AT2 cells were also significantly decreased compared to WT cells (Figure 2F, G). As these data point to a possible function of TRPV4 channels in secretion of SP-A and -D from AT2 cells, we used two established assays to probe a possible direct physical interaction with TRPV4 channels. SP-A and -D were co-immunoprecipitated after overexpression in HEK293 cells with antibodies specific for TRPV4 and vice versa (Figure 3A-D), while TRPC6 channels failed to coimmunoprecipitate SP-A

(Supplemental Figure E5). Moreover, using a Proximity ligation Assay a close interaction of both surfactant proteins with TRPV4 channels was detected in primary AT2 cells from WT, but not from TRPV4-/- mice (Figure 3E). However, this interaction was predominantly in inner cell compartments (Supplemental Figure E7). Therefore, TRPV4 might be essential for secretion of SP-A and SP-D by physically interacting in cell organelles and supporting translocation of both SPs to the plasma membrane by a still to be identified molecular mechanism.

As SP-A and -D are also produced in the tracheal bronchial region by club cells (43, 44), we utilized an ALI model to quantify protein levels in cell lysates of the pseudostratified epithelium and the mucous layer (Figure 4A, B). Again, production in epithelial cells was not changed in TRPV4-/- cells compared to WT control cells, while protein levels in the mucous layer were significantly reduced (Figure 4C-F). In a translational approach, we obtained human bronchial epithelial cells from three healthy donors to establish a human ALI model (Figure 5A, B) and down-regulated expression levels of TRPV4 channels by specific siRNAs (Supplemental Figure E8A, B). Similar to our results obtained in murine lung epithelial cells, SP-A and SP-D levels were not significantly changed in cell lysates, but SP-A levels were reduced in mucous layers (Figure 7A-D). Final numbers of club and goblet cells were not smaller, but differentiation of ciliated cells was reduced in the human ALI model (Figure 6B-F). The possible role of TRPV4 in differentiation of ciliated cells was a surprising, but interesting observation which warrants future investigations.

Reduced levels of SP-A and SP-D are clearly not due to a decreased number of AT2 cells in the murine alveolus (39) and/or club cells in the human bronchial region (Figure 6B, 7B). However, as a secondary finding we identified a role for TRPV4 channels in human basal cell differentiation to ciliated cells, which were significantly reduced in cell

numbers in the human ALI model (Figure 6B, F). As total cell numbers were not significantly different and the decrease of ciliated cells (Figure 6G) was not accompanied by a parallel large increase of progenitor cells including basal (Figure 6C) and club cells (Figure 6D), the absence of TRPV4 protein may not affect early commitment to the ciliated cell lineage but specifically affect differentiation to ciliated cells at a later stage prior to ciliogenesis.

In a previous study, TRPV4 channel expression was confirmed in murine ciliated cells and TRPV4-/- mice had a reduced ciliary beat frequency induced by ATP in comparison to WT controls (29). In the human respiratory tract, however, a reduced number of ciliated cells is expected if TRPV4 channels are not functional (Figure 6F) and might compromise mucociliary clearance.

Loss of SP-A and SP-D was already studied in SP-A and SP-D deficient mouse models. While these mice show no major changes in surfactant activity and normal lung function (52, 53), a complex immunological phenotype was apparent (reviewed in (7). SP-A-/- animals are more susceptible for infections by e.g. *Streptococcus* (54) and *RSV* (55), but also produced more TNF-α after application of LPS (56) in comparison to WT controls. SP-D deficient mice showed an increased number of activated foamy alveolar macrophages with high levels of reactive oxygen species (ROS) and matrix metalloproteinases (MMP), which might be responsible for an unprovoked progressive postnatal inflammation and the development of emphysema (53, 57). SP-A/SP-D double deficient mice mainly resemble the lung phenotype seen in SP-D-/- mice (58). We already described an emphysema like phenotype of the TRPV4-/- mouse model (39), which was also apparent in SP-C-deficient animals (59).

Surfactant secretion in producing cells is strongly dependent on intracellular Ca^{2+} levels (reviewed in (60)). Some authors propose TRPV2 channels as the main source

of Ca^{2+} influx into the cells, which was blocked by ruthenium red (61). But next to TRPV2, ruthenium red is also a potent blocker of TRPV4 channels, which can be activated by stretch and changes in osmolarity in the respiratory tract. However, as physical interaction occurs mostly in intracellular compartments (Supplemental Figure E7) and not at the plasma membrane, a mechanosensitive activation of TRPV4 channels at and Ca^{2+} influx near the plasma membrane is less likely. While we at this point can only speculate about an intracellular interaction of TRPV4 with SP-A and -D proteins in secretory vesicles of AT2 cells, a location and function of TRPV4 in organelles like mitochondria (62), nuclei (63) and the ER (64) was already reported. Splice variants of TRPV4 are specifically retained in the ER (64) and an Os9 protein interacts with the TRPV4 N-terminus to reduce plasma protein expression of this channel (65). Future studies need to further analyze the regulation of SP-A as well as SP-D secretion by TRPV4 channels in intracellular compartments of AT2 and club cells.

In summary, our data highlight novel essential functions of TRPV4 channels in SP-A and SP-D secretion. As outlined in the introduction, both SPs are linked to numerous immunological and pathophysiological processes in the respiratory tract including lung repair, asthma, IPF and inflammation (reviewed in (66)). Therefore, this TRPV4-deficient mouse model with reduced SP-A and SP-D secretion might not only result in a defective immune response against pathogens, but also in changes in asthma and IPF progression as well as lung repair and inflammation, which needs to be identified in future studies.

Acknowledgements

The authors thank Bettina Braun and Benedikt Kirmayer for excellent technical assistance and the Riken BioResource Center (RBR) as well as the Mutant Mouse Resource and Research Center (MMRRC) for providing the mouse models. This study was funded by the Deutsche Forschungsgemeinschaft (TRR 152, project 15 (TG), 16 (AD), GRK 2338, project 04 (AD) 10 (TG), and the German Center for Lung Research (DZL) (AD, C.S.-W., MG, TG).

Figure legends

Figure 1. Surfactant protein A (SP-A) and D (SP-D) levels in murine lung lysates and bronchoalveolar lavage (BAL) fluid of wild-type (WT) and TRPV4-deficient (TRPV4-/-) mice. (*A*) SP-A and (*B*) SP-D expression in whole mouse lungs was evaluated by immunoblotting of whole lung lysates from WT and TRPV4−/− mice. Values were normalized to vinculin (Vinculin) as loading control and are shown as % of WT. (*C*) Total lung volumes and (*D*) lung volumes normalized to body weights (lung volumes / body weight) of WT and TRPV4-/- mice. (*E*) SP-A and (*F*) SP-D expression in BAL fluid from mouse lungs of wild-type (WT) and TRPV4-deficient (TRPV4−/−) mice. Values were normalized to lung volumes / body weight. Data represent means + SEM from at least 6-12 mice each genotype. Significance between means was analyzed using two-tailed unpaired Student's t-test and is indicated as *** for $p<0.005$, ** for $p<0.01$ and * for $p<0.05$.

Figure 2. Surfactant protein A (SP-A) and D (SP-D) expression in murine alveolar type 2 (AT2) cells from wild-type (WT) and TRPV4-deficient (TRPV4-/-) mice. (*A*) AT2 cells after isolation from WT mice are stained with DAPI (blue) or (*B*) with a pro-surfactant protein C (pSP-C) antibody with secondary anti-rabbit IgG Alexa™488 (green). (*C*) Overlay of the two immunofluorescent images. (*D*) SP-A and (*E*) SP-D expression in AT2 cells was evaluated by immunoblotting of cell lysates from WT and TRPV4−/− mice. Values were normalized to β-actin (β-Actin) or vinculin (Vinculin) as loading control and are shown as % of WT. (*F*) SP-A and (*G*) SP-D levels in AT2 cell supernatants from WT and TRPV4−/− mice were quantified by ELISA. Data represent means + SEM from 3 different isolations containing 5 mice each (total WT = 15,

TRPV4-/- = 15). Significance between means was analyzed using two-tailed unpaired Student's t-test and is indicated as **** for p<0.001.

Figure 3. Surfactant protein A (SP-A) and D (SP-D) physically interact with TRPV4 channels in a heterologous overexpression system and primary AT2 cells. (*A*) HEK293 cells were transfected with SP-A flag (SP-A), TRPV4 (TRPV4), both (SP-A/TRPV4) cDNAs or mock (-). Proteins were co-immunoprecipitated with TRPV4 or flag antibody, separated by PAA gel electrophoresis and identified in a Western Blot by flag antibodies (Flag ab.). (*B*)HEK293 cells were transfected with SP-A flag (SP-A), TRPV4 (TRPV4), both (SP-A/TRPV4) cDNAs or mock (-). Proteins were co-immunoprecipitated with TRPV4 or flag antibody, separated by PAA gel electrophoresis and identified in a Western Blot by TRPV4 antibodies (TRPV4 ab.). (*C*) HEK293 cells were transfected with SP-D (SP-D), TRPV4 (TRPV4), both (SP-D/TRPV4) cDNAs or mock (-). Proteins were co-immunoprecipitated with TRPV4 or flag antibody, separated by PAA gel electrophoresis and identified in a Western Blot by SP-D antibodies (SP-D ab.). (*D*) HEK293 cells were transfected with SP-D (SP-D), TRPV4 (TRPV4), both (SP-D/TRPV4) cDNAs or mock (-). Proteins were co-immunoprecipitated with TRPV4 or flag antibody, separated by PAA gel electrophoresis and identified in a Western Blot by TRPV4 antibodies (TRPV4 ab.). (*E*) Fluorescent images from primary AT2 cells from wild-type (WT) and TRPV4-deficient mice (TRPV4-/-) after performing a Proximity ligation assay (PLA) using TRPV4 (TRPV4 ab.), SP-A (SP-A ab.), SP-D (SP-D ab.) antibodies or PLA-probes or antibodies (abs only) only.

Figure 4. SP-A and SP-D levels in cell lysates and mucous layers of an Air-Liquid-Interface (ALI) model with murine tracheal epithelial cells (mTEC) from wildtype (WT) and TRPV4-deficient (TRPV4-/-) mice. (*A*) Schematic presentation of the ALI model for differentiation of club and ciliated cells from mTEC. (*B*) Top view on the differentiated pseudostratified epithelium with a mucous layer 21 days after air-lift. (*C*) SP-A expression in cell lysates, cell lysates with the mucous layer and the mucous layer of WT and TRPV4-/- mTEC differentiated 21 days after air lift. Vinculin serves as loading controls for cell lysates. (*D*) Quantification of SP-A production in cell lysates and mucous layers of WT and TRPV4-/- mTEC differentiated 21 days after air lift. (*E*) SP-D expression in cell lysates, cell lysates with mucous layer and mucous layer of WT and TRPV4-/- mTEC differentiated 21 days after air lift. Vinculin served as loading controls for cell lysates. (*F*) Quantification of SP-D production in cell lysates and mucous layer of WT and TRPV4-/- mTEC differentiated 21 days after air lift. Data represent means + SEM from at least 3 cell isolations of each genotype. Significance between means was analyzed using two-dailed unpaired Student's t-test and is indicated as *** for $p<0.001$.

Figure 5. Differentiation of respiratory epithelial cells in an Air-Liquid-Interface (ALI) model with human bronchial epithelial cells (HBEC). (*A*) Schematic presentation of the ALI model from HBEC. Time points for transfection and analysis are marked. (*B*) Images from cross sections through Transwell™ inserts with attached cell layers 7, 14, 21 and 28 days after air lift. Appearance of cilia from day 14 on are marked by white arrows.

Figure 6. Immunofluorescence images and numbers of cells differentiated to a pseudostratified epithelium in an Air-Liquid-Interface (ALI) model with human bronchial epithelial cells (HBEC) with or without down-regulation of TRPV4

channels. (*A*) 3-D cross-section through a filter insert with differentiated cells stained with fluorescent-coupled antibodies against cell specific proteins as indicated or all nuclei with DAPI (blue). (*B*) Top views on filter inserts 7 and 28 days after air-lift. Naïve cells and cells transfected with control siRNAs (Ctrl. siRNA) or TRPV4 specific siRNAs (TRPV4 siRNA) are stained with fluorescent-coupled antibodies against cell specific proteins as indicated. (C) Percent (%) of basal cells in total cell counts during differentiation in an ALI model of untransfected (no siRNA) HBEC and of cells transfected with a control siRNA (Ctrl. siRNA) or a TRPV4 specific siRNA (TRPV4 siRNA). (*D*) Percent (%) of club cells in total cell counts during differentiation in an ALI model of untransfected (no siRNA) HBEC and of cells transfected with a control siRNA (Ctrl. siRNA) or a TRPV4 specific siRNA (TRPV4 siRNA). (*E*) Percent (%) of goblet cells in total cell counts during differentiation in an ALI model of untransfected (no siRNA) HBEC and of cells transfected with a control siRNA (Ctrl. siRNA) or a TRPV4 specific siRNA (TRPV4 siRNA). (*F*) Percent (%) of ciliated cells in total cell counts during differentiation in an ALI model of untransfected (no siRNA) HBEC and of cells transfected with a control siRNA (Ctrl. siRNA) or a TRPV4 specific siRNA (TRPV4 siRNA). (*G*) Total cell counts identified by DAPI staining of nuclei counts during differentiation in an ALI model of untransfected (no siRNA) HBEC and of cells transfected with a control siRNA (Ctrl. siRNA) or a TRPV4 specific siRNA (TRPV4 siRNA). Data represent means + SEM from 3 donors. Significance between means of cells transfected with control siRNA and TRPV4 specific siRNAs was analyzed using two-way ANOVA and indicated as **** for $p<0.0001$, ** for $p<0.01$ and * for $p<0.05$.

Figure 7. Surfactant protein A (SP-A) and D (SP-D) expression quantified by ELISA in an Air-Liquid-Interface (ALI) model with human bronchial epithelial cells (HBEC) in cell lysates and mucous layers after downregulation of TRPV4

channels. (*A*) SP-A expression in cell lysates from the ALI model 7, 14, 21 and 28 days after air-lift in untransfected (no siRNA) HBEC and cells transfected with a control siRNA (Ctrl. siRNA) or a TRPV4 specific siRNA (TRPV4 siRNA) 3 days before air lift. (*B*) SP-A expression in cell lysates from the ALI model 35 days after air-lift in untransfected (no siRNA) HBEC and cells transfected with a control siRNA (Ctrl. siRNA) or a TRPV4 specific siRNA (TRPV4 siRNA) at day 28 after air lift. (*C*) SP-A expression in the mucous layer of the ALI model 7, 14, 21 and 28 days after air-lift in untransfected (no siRNA) HBEC and cells transfected with a control siRNA (Ctrl. siRNA) or a TRPV4 specific siRNA (TRPV4 siRNA) 3 days before air lift. (*D*) SP-A expression in the mucous layer of the ALI model 35 days after air-lift in untransfected (no siRNA) HBEC and cells transfected with a control siRNA (Ctrl. siRNA) or a TRPV4 specific siRNA (TRPV4 siRNA) at day 28 after air lift. (*E*) SP-D expression in cell lysates from the ALI model 35 days after air-lift in untransfected (no siRNA) HBEC and cells transfected with a control siRNA (Ctrl. siRNA) or a TRPV4 specific siRNA (TRPV4 siRNA) at day 28 after air lift. Data present means + SEM from 3 different donors. Significance between means was analyzed using two-way ANOVA and is indicated as **** for $p<0.0001$ and ** for $p<0.01$.

References

1. Haagsman HP, and Diemel RV. Surfactant-associated proteins: functions and structural variation. *Comp Biochem Physiol A Mol Integr Physiol.* 2001;129(1):91-108.
2. Castillo-Sanchez JC, Cruz A, and Perez-Gil J. Structural hallmarks of lung surfactant: Lipid-protein interactions, membrane structure and future challenges. *Arch Biochem Biophys.* 2021;703:108850.
3. Vieira F, Kung JW, and Bhatti F. Structure, genetics and function of the pulmonary associated surfactant proteins A and D: The extra-pulmonary role of these C type lectins. *Ann Anat.* 2017;211:184-201.
4. Watson A, Madsen J, and Clark HW. SP-A and SP-D: Dual Functioning Immune Molecules With Antiviral and Immunomodulatory Properties. *Frontiers in immunology.* 2020;11:622598.
5. Jacob IB, Gemmiti A, Xiong W, Reynolds E, Nicholas B, Thangamani S, et al. Human surfactant protein A inhibits SARS-CoV-2 infectivity and alleviates lung injury in a mouse infection model. *Frontiers in immunology.* 2024;15:1370511.
6. Wright JR. Immunoregulatory functions of surfactant proteins. *Nat Rev Immunol.* 2005;5(1):58-68.
7. Milad N, and Morissette MC. Revisiting the role of pulmonary surfactant in chronic inflammatory lung diseases and environmental exposure. *Eur Respir Rev.* 2021;30(162).
8. Griese M, Steinecker M, Schumacher S, Braun A, Lohse P, and Heinrich S. Children with absent surfactant protein D in bronchoalveolar lavage have more frequently pneumonia. *Pediatr Allergy Immunol.* 2008;19(7):639-47.
9. Francisco D, Wang Y, Marshall C, Conway M, Addison KJ, Billheimer D, et al. Small Peptide Derivatives Within the Carbohydrate Recognition Domain of SP-A2 Modulate Asthma Outcomes in Mouse Models and Human Cells. *Frontiers in immunology.* 2022;13:900022.
10. Garcia-Fojeda B, Minutti CM, Montero-Fernandez C, Stamme C, and Casals C. Signaling Pathways That Mediate Alveolar Macrophage Activation by Surfactant Protein A and IL-4. *Frontiers in immunology.* 2022;13:860262.
11. Coya JM, Fraile-Agreda V, de Tapia L, Garcia-Fojeda B, Saenz A, Bengoechea JA, et al. Cooperative action of SP-A and its trimeric recombinant fragment with polymyxins against Gram-negative respiratory bacteria. *Frontiers in immunology.* 2022;13:927017.
12. Ganguly K, Kishore U, Metkari SM, and Madan T. Immunomodulatory Role of Surfactant Protein-D in a Transgenic Adenocarcinoma of Mouse Prostate (TRAMP) Model. *Frontiers in immunology.* 2022;13:930449.
13. Wang Q, Wang Q, Zhao Z, Fan J, Qin L, Alexander DB, et al. Surfactant Proteins A/D-CD14 on Alveolar Macrophages Is a Common Pathway Associated With Phagocytosis of Nanomaterials and Cytokine Production. *Frontiers in immunology.* 2021;12:758941.
14. Depicolzuane LC, Roberts CM, Thomas NJ, Anderson-Fears K, Liu D, Barbosa JPP, et al. Hydrophilic But Not Hydrophobic Surfactant Protein Genetic Variants Are Associated With Severe Acute Respiratory Syncytial Virus Infection in Children. *Frontiers in immunology.* 2022;13:922956.
15. Abbasi A, Chen C, Gandhi CK, Wu R, Pardo A, Selman M, et al. Single Nucleotide Polymorphisms (SNP) and SNP-SNP Interactions of the Surfactant Protein Genes Are Associated With Idiopathic Pulmonary Fibrosis in a Mexican Study Group; Comparison With Hypersensitivity Pneumonitis. *Frontiers in immunology.* 2022;13:842745.
16. Wong CJ, Akiyama J, Allen L, and Hawgood S. Localization and developmental expression of surfactant proteins D and A in the respiratory tract of the mouse. *Pediatr Res.* 1996;39(6):930-7.
17. Bustamante-Marin XM, and Ostrowski LE. Cilia and Mucociliary Clearance. *Cold Spring Harb Perspect Biol.* 2017;9(4).
18. Crouch E, and Wright JR. Surfactant proteins a and d and pulmonary host defense. *Annu Rev Physiol.* 2001;63:521-54.

19. Zhang M, Ma Y, Ye X, Zhang N, Pan L, and Wang B. TRP (transient receptor potential) ion channel family: structures, biological functions and therapeutic interventions for diseases. *Signal Transduct Target Ther.* 2023;8(1):261.
20. Muller I, Alt P, Rajan S, Schaller L, Geiger F, and Dietrich A. Transient Receptor Potential (TRP) Channels in Airway Toxicity and Disease: An Update. *Cells.* 2022;11(18).
21. Nilius B, and Szallasi A. Transient receptor potential channels as drug targets: from the science of basic research to the art of medicine. *Pharmacological reviews.* 2014;66(3):676-814.
22. Dietrich A, Steinritz D, and Gudermann T. Transient receptor potential (TRP) channels as molecular targets in lung toxicology and associated diseases. *Cell Calcium.* 2017;67:123-37.
23. Hellwig N, Albrecht N, Harteneck C, Schultz G, and Schaefer M. Homo- and heteromeric assembly of TRPV channel subunits. *Journal of cell science.* 2005;118(Pt 5):917-28.
24. Kottgen M, Buchholz B, Garcia-Gonzalez MA, Kotsis F, Fu X, Doerken M, et al. TRPP2 and TRPV4 form a polymodal sensory channel complex. *J Cell Biol.* 2008;182(3):437-47.
25. Liedtke W, Choe Y, Marti-Renom MA, Bell AM, Denis CS, Sali A, et al. Vanilloid receptor-related osmotically activated channel (VR-OAC), a candidate vertebrate osmoreceptor. *Cell.* 2000;103(3):525-35.
26. Strotmann R, Harteneck C, Nunnenmacher K, Schultz G, and Plant TD. OTRPC4, a nonselective cation channel that confers sensitivity to extracellular osmolarity. *Nat Cell Biol.* 2000;2(10):695-702.
27. Hill-Eubanks DC, Gonzales AL, Sonkusare SK, and Nelson MT. Vascular TRP channels: performing under pressure and going with the flow. *Physiology (Bethesda).* 2014;29(5):343-60.
28. Marziano C, Hong K, Cope EL, Kotlikoff MI, Isakson BE, and Sonkusare SK. Nitric Oxide-Dependent Feedback Loop Regulates Transient Receptor Potential Vanilloid 4 (TRPV4) Channel Cooperativity and Endothelial Function in Small Pulmonary Arteries. *J Am Heart Assoc.* 2017;6(12).
29. Lorenzo IM, Liedtke W, Sanderson MJ, and Valverde MA. TRPV4 channel participates in receptor-operated calcium entry and ciliary beat frequency regulation in mouse airway epithelial cells. *Proc Natl Acad Sci U S A.* 2008;105(34):12611-6.
30. Li J, Kanju P, Patterson M, Chew WL, Cho SH, Gilmour I, et al. TRPV4-mediated calcium influx into human bronchial epithelia upon exposure to diesel exhaust particles. *Environ Health Perspect.* 2011;119(6):784-93.
31. Henry CO, Dalloneau E, Perez-Berezo MT, Plata C, Wu Y, Guillon A, et al. In vitro and in vivo evidence for an inflammatory role of the calcium channel TRPV4 in lung epithelium: Potential involvement in cystic fibrosis. *American journal of physiology Lung cellular and molecular physiology.* 2016;311(3):L664-75.
32. Goldenberg NM, Ravindran K, and Kuebler WM. TRPV4: physiological role and therapeutic potential in respiratory diseases. *Naunyn Schmiedebergs Arch Pharmacol.* 2015;388(4):421-36.
33. Xia Y, Fu Z, Hu J, Huang C, Paudel O, Cai S, et al. TRPV4 channel contributes to serotonin-induced pulmonary vasoconstriction and the enhanced vascular reactivity in chronic hypoxic pulmonary hypertension. *Am J Physiol Cell Physiol.* 2013;305(7):C704-15.
34. Goldenberg NM, Wang L, Ranke H, Liedtke W, Tabuchi A, and Kuebler WM. TRPV4 Is Required for Hypoxic Pulmonary Vasoconstriction. *Anesthesiology.* 2015;122(6):1338-48.
35. Rahaman SO, Grove LM, Paruchuri S, Southern BD, Abraham S, Niese KA, et al. TRPV4 mediates myofibroblast differentiation and pulmonary fibrosis in mice. *J Clin Invest.* 2014;124(12):5225-38.
36. Dietrich A. Modulators of Transient Receptor Potential (TRP) Channels as Therapeutic Options in Lung Disease. *Pharmaceuticals (Basel).* 2019;12(1).
37. Mizuno A, Matsumoto N, Imai M, and Suzuki M. Impaired osmotic sensation in mice lacking TRPV4. *Am J Physiol Cell Physiol.* 2003;285(1):C96-101.

38. Suzuki M, Mizuno A, Kodaira K, and Imai M. Impaired pressure sensation in mice lacking TRPV4. *J Biol Chem.* 2003;278(25):22664-8.
39. Weber J, Rajan S, Schremmer C, Chao YK, Krasteva-Christ G, Kannler M, et al. TRPV4 channels are essential for alveolar epithelial barrier function as protection from lung edema. *JCI Insight.* 2020;5(20).
40. Osanai K, Tsuchihara C, Hatta R, Oikawa T, Tsuchihara K, Iguchi M, et al. Pulmonary surfactant transport in alveolar type II cells. *Respirology.* 2006;11 Suppl:S70-3.
41. Rooney SA. Regulation of surfactant secretion. *Comp Biochem Physiol A Mol Integr Physiol.* 2001;129(1):233-43.
42. Soderberg O, Gullberg M, Jarvius M, Ridderstrale K, Leuchowius KJ, Jarvius J, et al. Direct observation of individual endogenous protein complexes in situ by proximity ligation. *Nature methods.* 2006;3(12):995-1000.
43. Madsen J, Tornoe I, Nielsen O, Koch C, Steinhilber W, and Holmskov U. Expression and localization of lung surfactant protein A in human tissues. *American journal of respiratory cell and molecular biology.* 2003;29(5):591-7.
44. Madsen J, Kliem A, Tornoe I, Skjodt K, Koch C, and Holmskov U. Localization of lung surfactant protein D on mucosal surfaces in human tissues. *J Immunol.* 2000;164(11):5866-70.
45. You Y, and Brody SL. Culture and differentiation of mouse tracheal epithelial cells. *Methods Mol Biol.* 2013;945:123-43.
46. Rayner RE, Makena P, Prasad GL, and Cormet-Boyaka E. Optimization of Normal Human Bronchial Epithelial (NHBE) Cell 3D Cultures for in vitro Lung Model Studies. *Scientific reports.* 2019;9(1):500.
47. Adams TS, Schupp JC, Poli S, Ayaub EA, Neumark N, Ahangari F, et al. Single-cell RNA-seq reveals ectopic and aberrant lung-resident cell populations in idiopathic pulmonary fibrosis. *Sci Adv.* 2020;6(28):eaba1983.
48. Schamberger AC, Staab-Weijnitz CA, Mise-Racek N, and Eickelberg O. Cigarette smoke alters primary human bronchial epithelial cell differentiation at the air-liquid interface. *Scientific reports.* 2015;5:8163.
49. Mastalerz M, Dick E, Chakraborty A, Hennen E, Schamberger AC, Schroppel A, et al. Validation of in vitro models for smoke exposure of primary human bronchial epithelial cells. *American journal of physiology Lung cellular and molecular physiology.* 2022;322(1):L129-L48.
50. Simmons S, Erfinanda L, Bartz C, and Kuebler WM. Novel mechanisms regulating endothelial barrier function in the pulmonary microcirculation. *J Physiol.* 2018.
51. Rajan S, Schremmer C, Weber J, Alt P, Geiger F, and Dietrich A. Ca(2+) Signaling by TRPV4 Channels in Respiratory Function and Disease. *Cells.* 2021;10(4).
52. Korfhagen TR, Bruno MD, Ross GF, Huelsman KM, Ikegami M, Jobe AH, et al. Altered surfactant function and structure in SP-A gene targeted mice. *Proc Natl Acad Sci U S A.* 1996;93(18):9594-9.
53. Korfhagen TR, Sheftelyevich V, Burhans MS, Bruno MD, Ross GF, Wert SE, et al. Surfactant protein-D regulates surfactant phospholipid homeostasis in vivo. *J Biol Chem.* 1998;273(43):28438-43.
54. LeVine AM, Bruno MD, Huelsman KM, Ross GF, Whitsett JA, and Korfhagen TR. Surfactant protein A-deficient mice are susceptible to group B streptococcal infection. *J Immunol.* 1997;158(9):4336-40.
55. LeVine AM, Gwozdz J, Stark J, Bruno M, Whitsett J, and Korfhagen T. Surfactant protein-A enhances respiratory syncytial virus clearance in vivo. *J Clin Invest.* 1999;103(7):1015-21.
56. Borron P, McIntosh JC, Korfhagen TR, Whitsett JA, Taylor J, and Wright JR. Surfactant-associated protein A inhibits LPS-induced cytokine and nitric oxide production in vivo. *American journal of physiology Lung cellular and molecular physiology.* 2000;278(4):L840-7.

57. Wert SE, Yoshida M, LeVine AM, Ikegami M, Jones T, Ross GF, et al. Increased metalloproteinase activity, oxidant production, and emphysema in surfactant protein D gene-inactivated mice. *Proc Natl Acad Sci U S A.* 2000;97(11):5972-7.
58. Hawgood S, Ochs M, Jung A, Akiyama J, Allen L, Brown C, et al. Sequential targeted deficiency of SP-A and -D leads to progressive alveolar lipoproteinosis and emphysema. *American journal of physiology Lung cellular and molecular physiology.* 2002;283(5):L1002-10.
59. Glasser SW, Detmer EA, Ikegami M, Na CL, Stahlman MT, and Whitsett JA. Pneumonitis and emphysema in sp-C gene targeted mice. *J Biol Chem.* 2003;278(16):14291-8.
60. Dietl P, Haller T, and Frick M. Spatio-temporal aspects, pathways and actions of Ca(2+) in surfactant secreting pulmonary alveolar type II pneumocytes. *Cell Calcium.* 2012;52(3-4):296-302.
61. Fois G, Wittekindt O, Zheng X, Felder ET, Miklavc P, Frick M, et al. An ultra fast detection method reveals strain-induced Ca(2+) entry via TRPV2 in alveolar type II cells. *Biomech Model Mechanobiol.* 2012;11(7):959-71.
62. Acharya TK, Kumar A, Kumar S, and Goswami C. TRPV4 interacts with MFN2 and facilitates endoplasmic reticulum-mitochondrial contact points for Ca(2+)-buffering. *Life sciences.* 2022;310:121112.
63. Mendez-Gomez S, Espadas-Alvarez H, Ramirez-Rodriguez I, Dominguez-Malfavon L, and Garcia-Villegas R. The amino-terminal domain of TRPV4 channel is involved in its trafficking to the nucleus. *Biochem Biophys Res Commun.* 2022;592:13-7.
64. Arniges M, Fernandez-Fernandez JM, Albrecht N, Schaefer M, and Valverde MA. Human TRPV4 channel splice variants revealed a key role of ankyrin domains in multimerization and trafficking. *J Biol Chem.* 2006;281(3):1580-6.
65. Wang Y, Fu X, Gaiser S, Kottgen M, Kramer-Zucker A, Walz G, et al. OS-9 regulates the transit and polyubiquitination of TRPV4 in the endoplasmic reticulum. *J Biol Chem.* 2007;282(50):36561-70.
66. Madan T, and Thielens NM. Editorial: Updates on the role of surfactant proteins A and D in innate immune responses. *Frontiers in immunology.* 2022;13:1113210.

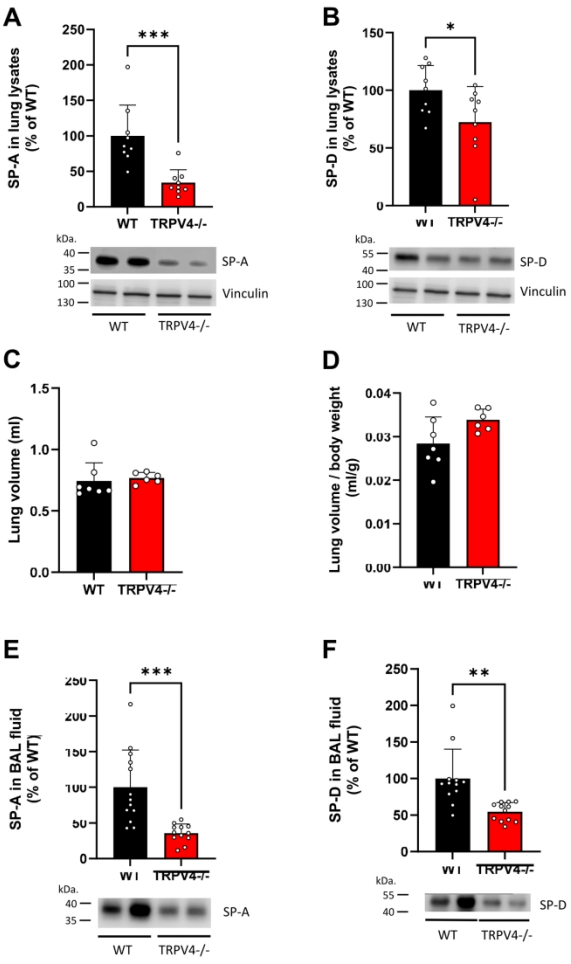

Figure 1

209x297mm (300 x 300 DPI)

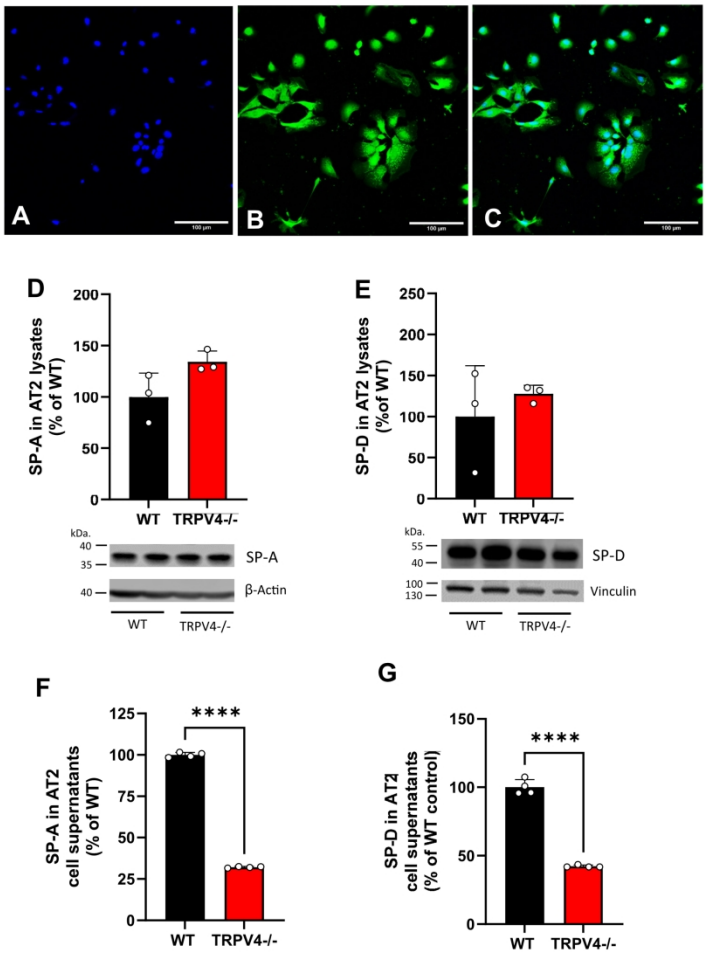

Figure 2

209x297mm (300 x 300 DPI)

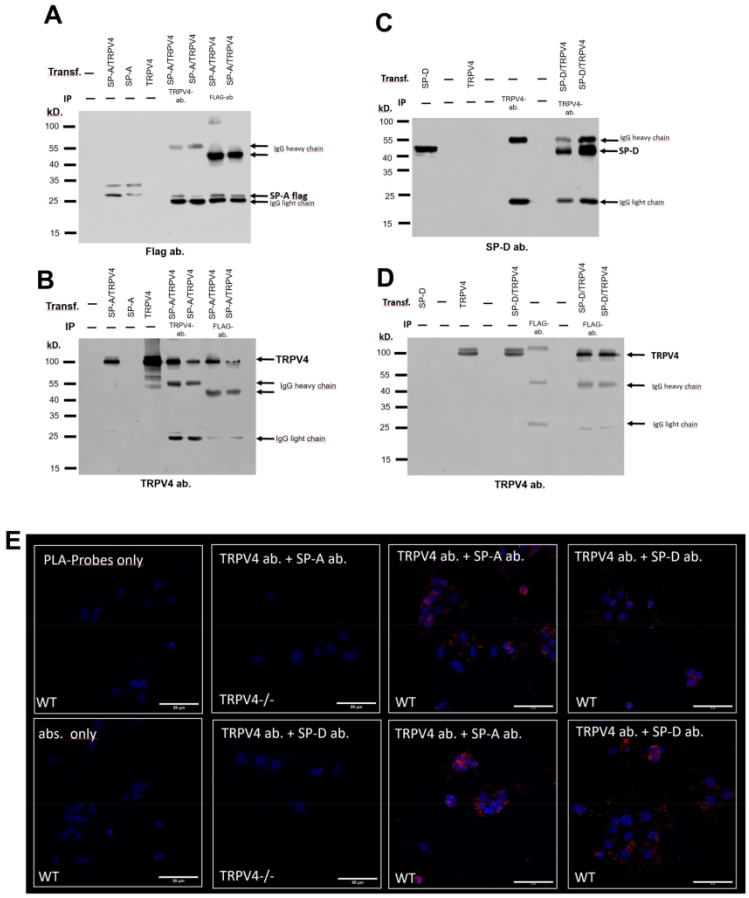

Figure 3

209x297mm (300 x 300 DPI)

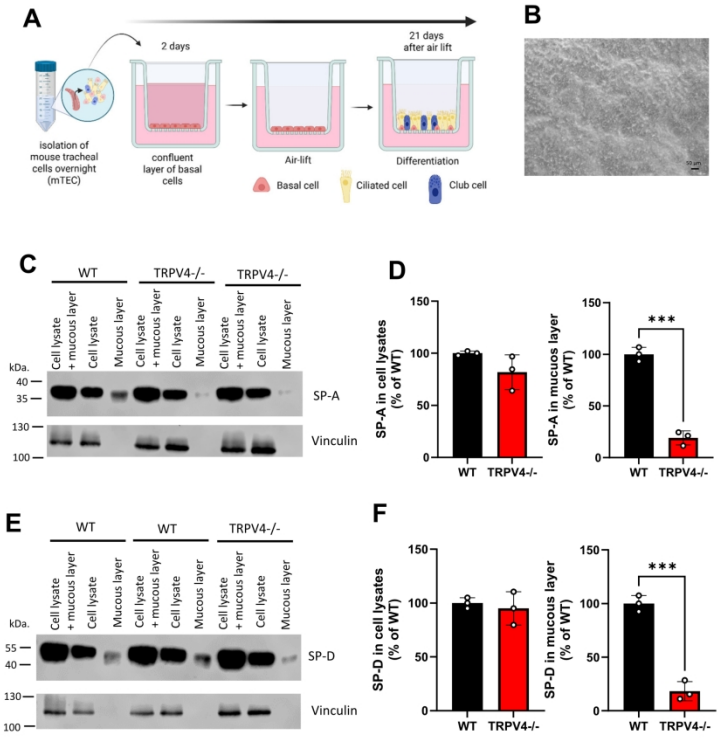

Figure 4

209x297mm (300 x 300 DPI)

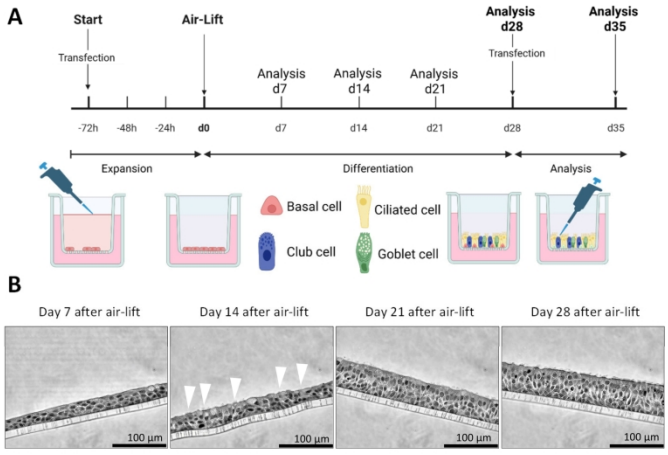

Figure 5

209x297mm (300 x 300 DPI)

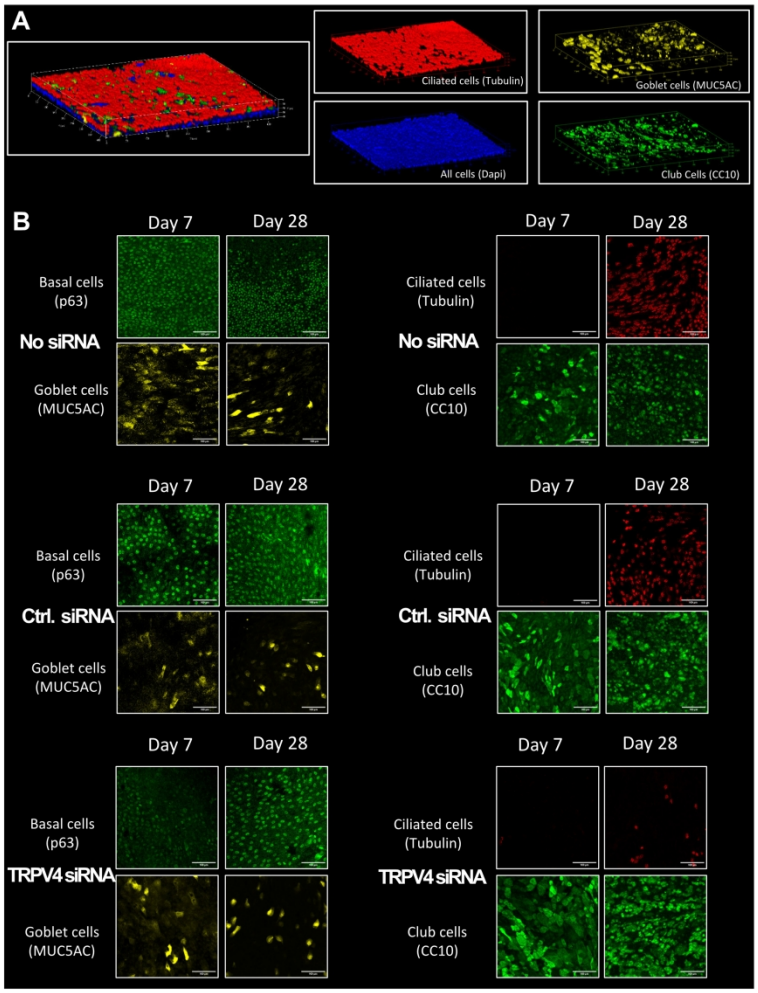

Figure 6

209x297mm (300 x 300 DPI)

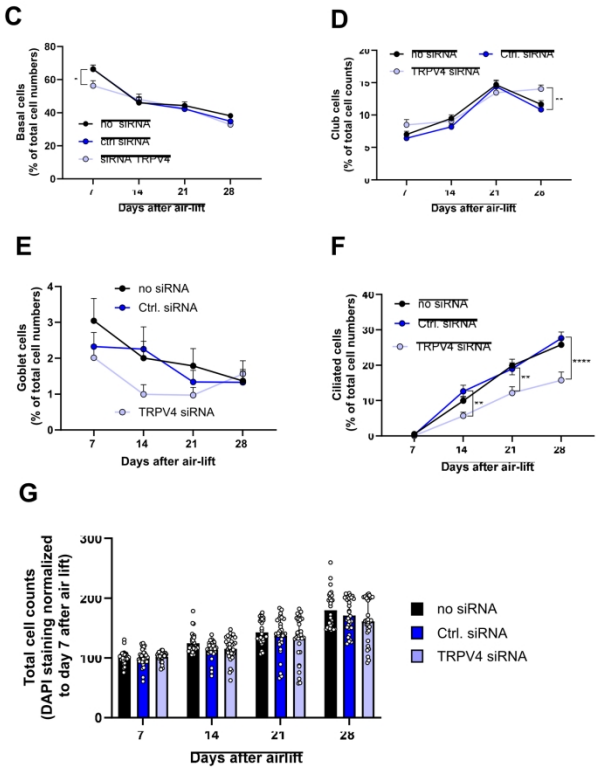

Figure 6 ctd.

209x297mm (300 x 300 DPI)

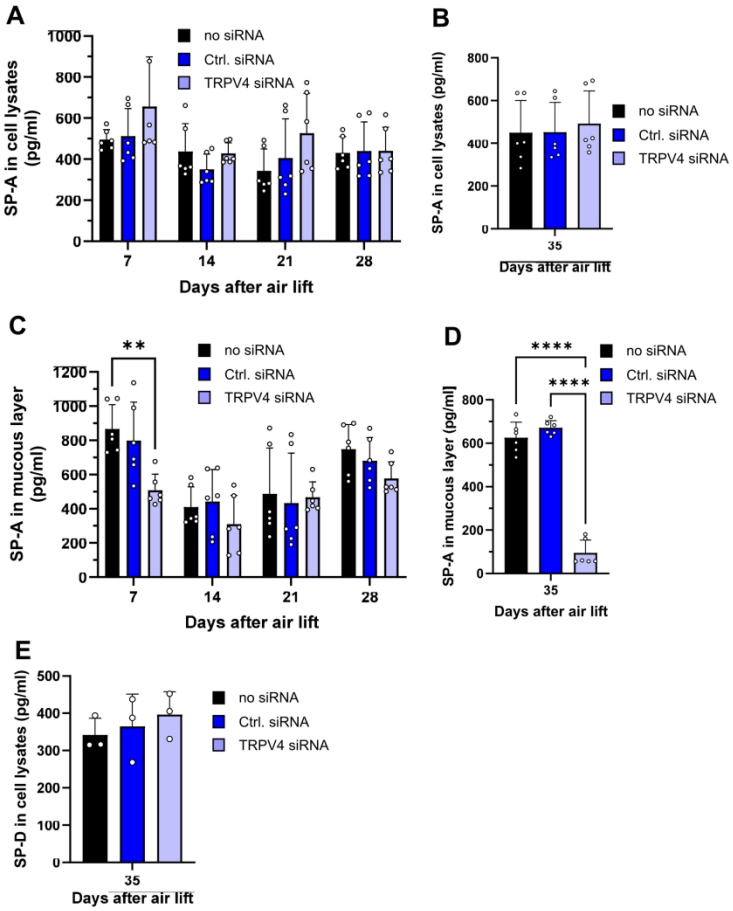

Figure 7

209x297mm (300 x 300 DPI)